

A tunable mode-locked ytterbium-doped fiber laser based on nonlinear Kerr beam clean-up effect

Shanchao Ma,¹ Baofu Zhang,^{2,*} Qiurun He,¹ Jing Guo,³ and Zhongxing Jiao^{1,*}

¹*School of Physics, Sun Yat-sen University, Guangzhou 510275, China*

²*School of Materials Science and Engineering, Dongguan University of Technology, Dongguan 523808, China*

³*School of Opto-Electronics, Beijing Institute of Technology, Beijing 100081, China*

*Corresponding author: zhanabf5@mail.sysu.edu.cn, jiaozhx@mail.sysu.edu.cn

Abstract: We demonstrate a novel approach to achieve tunable ultrashort pulses from an all-fiber mode-locked laser with a saturable absorber based on nonlinear Kerr beam clean-up effect. This saturable absorber was formed by a single-mode fiber spliced to a commercial graded-index multimode fiber, and its tunable band-pass filter effect has been studied by an original numerical model. By adjusting the bending condition of graded-index multimode fiber, the laser could produce dissipative soliton pulses with their central wavelength tunable from 1033 nm to 1063 nm. The pulse width of output laser could be compressed externally to 791 fs, and the signal to noise ratio of its radio frequency spectrum was measured to be 75.5 dB. This work provides a new idea for the design of tunable mode-locked laser which can be used as an attractive light source in optical communication system.

1. Introduction

Wavelength tunable lasers are widely used in optical communication [1], detection [2], and remote sensing [3]. Compared to tunable continuous-wave lasers, tunable mode-locked lasers can generate ultra-short pulses with high peak power and wide bandwidth that enable many important advances, such as high-sensitivity optical absorption measurement [4], multi photon microscopy [5], and super-continuum light source used in dense wavelength division multiplexing [6]. Moreover, due to the high conversion efficiency, low temperature sensitivity and compact structure of fiber lasers, tunable mode-locked fiber lasers [7-10] have attracted extensive research interest.

Up to date, there are several typical approaches to achieve the tunability of mode-locked fiber lasers. The most common method is to add a tunable spectral filter into the laser cavity [7-10]. However, some of these filters achieve wavelength tuning by rotating or tilting the optical elements [7,8], which will cause additional loss and affect integration when they are coupled with optical fiber. Although chirped fiber Bragg gratings have been used to achieve tunable output [9], the tuning range is limited to a few nanometers, and its narrow bandwidth is not suitable for sub picosecond pulse generation. Fourier domain programmable optical processor can also be used as spectral filter [10], but it was based on a two-dimensional liquid-crystal-on silicon array which cannot be easy to construct. Therefore, in order to meet the requirements of emerging applications, more attention should be paid to find out a simple and reliable solution for tunable mode-locked fiber lasers.

Nonlinear Kerr beam cleanup (NL-KBC) effect occurs when high-power laser propagates in the graded-index multimode fiber (GIMF). With the increasing laser power or longer fiber length, energy of high-order modes (HOMs) can be irreversibly coupled into the fundamental mode, where nonlinear Kerr effect is the driving mechanism [11, 12]. Based on this NL-KBC effect, we have constructed all-fiber saturable absorbers (SAs) with the structure of a long graded-index multimode fiber (GIMF) spliced to a short single-mode fiber (SMF) in our previous work [13, 14]. We experimentally investigated characteristics of these SAs [13], and then demonstrated a mode-locked ytterbium-doped fiber laser using one of them [14]. For this fiber laser, the stable and self-starting mode-locking operation can be obtained, but the lasing performance would be different if the bending condition of the GIMF was changed. After preliminary theoretical and experimental studies, we found that the bending of GIMF in the laser might lead to different transverse mode distribution of the beam with different wavelengths, resulting in a band-pass filter characteristic along with the NL-KBC effect. Therefore, it may be a new approach to achieve wavelength-tunable output in the mode-locked fiber lasers.

In this paper, an all-fiber wavelength-tunable mode-locked laser based on NL-KBC effect is demonstrated, and its tuning mechanism is theoretically studied by a numerical model. For this laser, stable mode-locked operation with a wide tunable range from 1033 nm to 1063 nm can be obtained; the output pulse duration can be compressed externally to 791 fs. The wavelength tuning is easy to be achieved by adjusting the bending condition of graded-index multimode fiber, and its performances are in good agreement with the numerical model.

2. Theoretical model and numerical simulation

In this section, we will investigate the band-pass filter effect and saturable absorption property of an SA based on NL-KBC by a numerical model. The model may become too complicated to achieve solutions if the NL-KBC effect and multimode-coupling introduced by the bending condition act together along the length of GIMF. Therefore, a simplified model is used here to simulate the output laser characteristics after it propagates through the SA. In this model, the SA can be divided into four parts which are centrally aligned (shown in Fig. 1): an input SMF, a short GIMF segment with a small radius of curvature which can be adjusted by translation stages, a long and straight GIMF segment, and an output SMF. A commercial GIMF (Nufern GR-50/125-23HTA) is used here; both input and output SMFs have the same type and specification (Nufern, Hi1060-XP). It is assumed that only the multimode-coupling effect introduced by the bending condition is considered in the short GIMF segment, while dispersion and nonlinear effects are considered in the long GIMF segment. The bending condition here refers to the curved length and curvature radius. Since the mode field diameter of this SMF is close to the fundamental-mode (FM) diameter of GIMF, we

can obtain approximate solutions by assuming that all laser energy from the input SMF will be transferred to the excited FM energy in the GIMF, while only the FM energy at the end of GIMF can be coupled into the output SMF. With this approximation, the transmittance of this SA can be defined as the ratio of FM energy at the end of GIMF to the launched laser energy from the input SMF. The main theoretical method of our model and some important assumptions are listed at the flowchart in Fig. 1(b); their processes are detailed in following sections.

In the short GIMF segment, the influences of bending condition on the transverse mode distribution of laser beam with different wavelengths are studied. For qualitative analysis, the bending of GIMF can greatly affect mode propagation constants and hence the coupling coefficients between transverse modes of laser beam [15]. Besides, mode propagation constants also depend on the laser wavelength. Therefore, when a FM laser beam propagates through a curved GIMF, high-order modes can be excited; the bending condition and laser wavelength will have important influences on the output transverse mode distribution. In order to figure out these influences, numerical simulations are performed by solving the wave coupling equation through a curved GIMF; this numerical method is similar to that detailed in Sohn's work [16]. First, the transverse eigenmodes and their intensity profiles of GIMF can be obtained by numerically solving the waveguide eigen equation using a difference equation representation of the differential equation. Then, local transverse mode fields are matched at a succession of infinitesimal corner bends to calculate mode coupling induced by the constant radius bending. Finally, the transverse mode distribution, especially the proportion of FM energy versus laser wavelength, propagation distance or curvature radius, can be obtained at the end of GIMF. In this simulation, the length of short GIMF segment is set to be 40 mm with its curved length of 10-40 mm and a curvature radius of 2-10 mm according to our previous work [14]. Moreover, it is assumed that the propagating laser beam is monochromatic, but the dispersion and nonlinear effects are not considered as mentioned above. Only linear-polarized (LP) modes are considered in this simulation; the energy proportion of LP₀₁ mode (fundamental mode) at the end of short GIMF segment with different bending conditions is shown in Fig. 2. For specific bending condition, the energy proportion of LP₀₁ mode varies with the laser wavelength. Moreover, with smaller curvature radius and longer curved length, more peaks with similar energy proportion of LP₀₁ mode can be found. These numerical results are in good agreement with the qualitative analysis mentioned above. As a result, the transverse mode distribution and the proportion of LP₀₁ mode energy versus wavelength at the end of short GIMF segment will be served as the input condition for numerical simulations in the long GIMF segment.

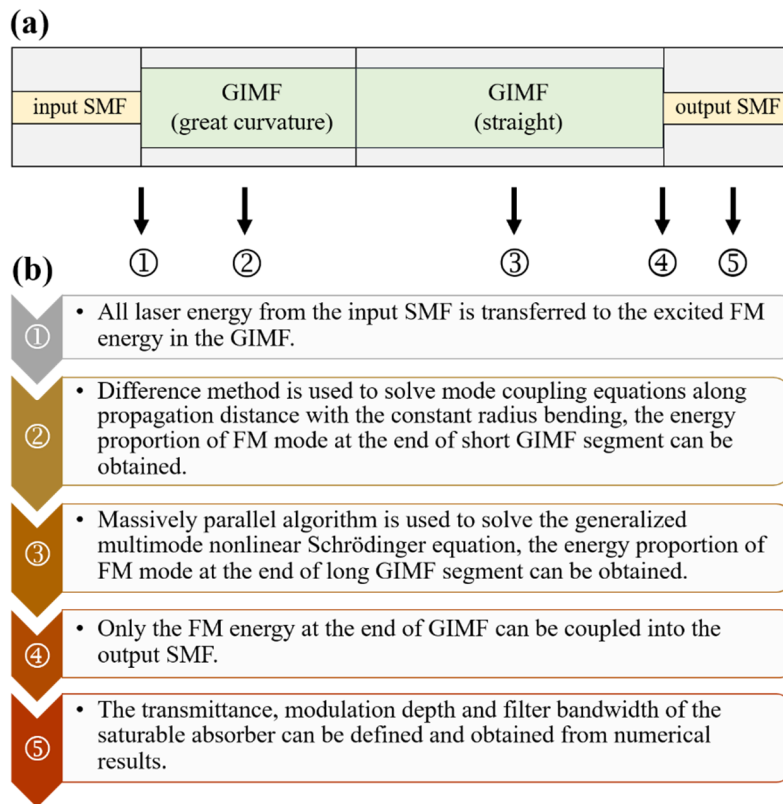


Fig. 1. (a) The structure of a saturable absorber based on nonlinear Kerr beam cleanup effect and (b) the flowchart of our numerical model. SMF: single-mode fiber; GIMF: graded-index multimode fiber; FM: fundamental-mode.

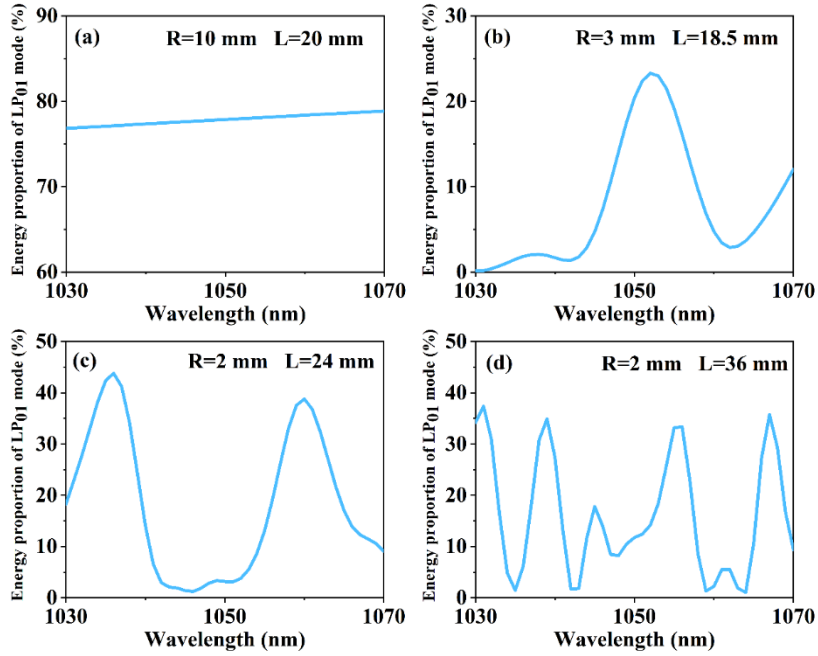


Fig. 2. The simulated proportion of LP₀₁ mode at the end of the short graded-index multimode fiber segment with different bending conditions. R: radius of the curvature; L: the curved length.

In the long GIMF segment, the influences of input condition on the output laser characteristics are studied. Since the main issue here is multimode nonlinear optical pulse propagation, numerical simulations are performed by solving a generalized multimode nonlinear Schrödinger equation (GMMNLSE) using massively parallel algorithm (MPA). The MPA numerical solver we used is the same as that reported by Logan G. Wright et al. [17], and its details have also been systematically studied in this reference. In our numerical model, only the first ten LP modes are considered. Moreover, the effects of self-phase modulation, stimulated Raman scattering, and the first five order dispersion are included in the simulations, but the random linear distortions such as random radius perturbation and random index perturbation introduced by the imperfections or bending of GIMF are not included. According to our previous work [14], the length of long GIMF segment is set to be 2 m, and the input laser pulse has a duration of 250 fs with different pulse energy and central wavelength. Besides, as shown in Fig. 2(a), the bending condition with a curvature radius larger than 10 mm has little influence on the output transverse mode distribution, and thus the long GIMF segment is assumed to be straight in this model. For the situation of short GIMF segment with 18.5-mm curved length and 3-mm curvature radius, as shown in Fig. 2(b), the energy proportion of LP₀₁ mode versus wavelength is simple and clear with a single peak at 1052 nm. Therefore, in the following simulations, this situation is chosen as the input condition of long GIMF segment. First, high-energy multimode laser pulse propagation through the long GIMF segment is studied. When the laser pulse energy is set to be 50 nJ and its wavelength is 1052 nm, the evolution of laser transverse mode distribution along the GIMF is shown in Fig. 3(a). During the propagation, the proportion of LP₀₁ mode first increases from 23% to 43%, and then gradually keeps stable at 33%; most of HOMs have a lower proportion at the end of GIMF. Therefore, part of HOM energy is irreversibly coupled into the fundamental mode, which indicates the NL-KBC effect occurs in this case. Then, we focus on the optical properties of this SA which depend on output laser characteristics after it propagates through this long GIMF

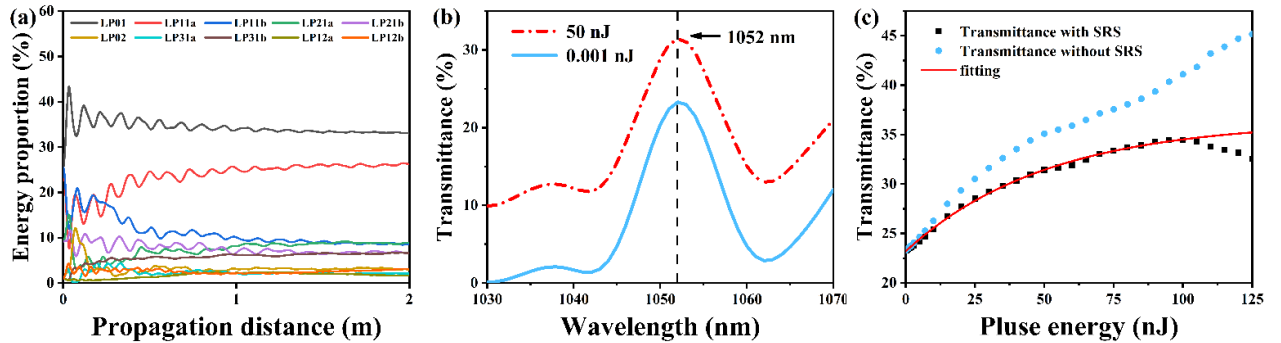


Fig. 3. Numerical results for the saturable absorber: (a) the evolution of modal energy proportion along the long GIMF segment when the laser wavelength is 1052 nm; (b) the transmittance of saturable absorber versus input laser wavelength when the pulse energy is 50 nJ (red line) and 0.001 nJ (blue line); (c) the transmittance of saturable absorber versus input pulse energy when the laser wavelength is 1052 nm.

segment. As mentioned above, the transmittance of this SA can be defined as the ratio of FM energy at the end of GIMF to the launched laser energy from the input SMF. The relationship between transmittance of the SA and laser wavelength is presented in Fig. 3(b); the cases of input laser beam with high pulse energy (50 nJ) and low pulse energy (0.001 nJ) are both considered. As shown in Fig. 3(b), the transmittance of SA versus wavelength have a similar shape with the energy proportion of LP₀₁ mode as shown in Fig. 2(b), which results in a band-pass filtering effect. This band-pass filter can be tunable since its central wavelength and bandwidth can be adjusted by changing the bending condition of short GIMF segment and hence the input transverse mode distribution of long GIMF segment. In addition, the transmittance with higher input pulse energy (red line) is higher than that with lower energy (blue line) at each wavelength, which confirms the saturable absorption effect of this SA.

Finally, in order to further evaluate optical properties of the SA, its transmittance under different input pulse energy is studied and the numerical results are presented in Fig. 3(c); the laser wavelength is chosen to be 1052 nm which is the central wavelength of band-pass filter effect. As shown in Fig. 3(c), the transmittance first grows monotonically as the input pulse energy increased and then decrease when the pulse energy is higher than 95 nJ. The decrease of transmittance may be caused by stimulated Raman scattering (SRS) which can lead to the serious dissipation of propagating laser power [12]. This assumption is also supported by the monotonically increasing transmittance when SRS is not included in the simulation. In order to evaluate the modulation depth and saturation intensity of this SA, the transmittance curve before the decrease can be fitted by

$$T = T_0 + q \cdot \left[1 - \exp\left(-\frac{I}{I_{SAT}}\right) \right], \quad (1)$$

where T is the transmittance, T_0 is the initial transmittance, q can be defined as the modulation depth, I and I_{SAT} are the input and saturation intensity, respectively. As shown in Fig. 3(c), the curve fits well with the numerical results; the initial transmittance, modulation depth and saturation intensity are fitted to be 23.2 %, 13.14 % and 50.75 nJ, respectively. These results further ensure the saturable absorption effect of the SA.

In conclusion of this section, a numerical model is used to study the optical properties of the SA based on NL-KBC effect. The simulation results indicate that the bending condition plays an important role in the transverse mode distribution of GIMF and hence the transmittance of SA. Saturable absorption and band-pass filter effect with tunable central wavelength of the SA can be achieved with specific bending condition of GIMF when the NL-KBC occurs. Therefore, this SA may be promising for constructing tunable mode-locked lasers.

3. Experiments and results

In order to verify the tunable band-pass effect of the SA based on NL-KBC, we built up a mode-locked ytterbium-doped fiber laser with this SA. As shown in Fig. 4, the configuration of the laser is similar to that demonstrated in our previous work [14] except the polarization independent isolator (PI-ISO) used in the cavity had a wide bandwidth (>50 nm). In this laser, a 976-nm laser diode was used as the pump source, and its pump power was coupled into an ytterbium-doped fiber (Yb1200-4/125, LIEKKI) through a commercial wavelength division multiplexer (WDM). The length of this gain fiber was chosen to be 0.3 m in order to reduce the mode-locked threshold and increase the output power. 10 % of the mode-locked laser was output from a coupler after the ytterbium-doped fiber. The output port of coupler was connected with an isolator to prevent the influence of reflected light on the laser performance. The function of PI-ISO was to ensure the unidirectional operation of laser and eliminate the possibility of nonlinear-polarization-evolution mode locking. Two polarization controllers (PCs) were used to optimize intracavity birefringence in order to achieve stable mode-locked state. The SA was the same as what we mentioned in the simulation section, and it was placed between the two PCs. The bending condition of short GIMF segment can be adjusted by two translation stages. All single-mode passive fibers used in this laser were the same type (HI-1060, Corning); the total cavity length was measured to be about 7.4 m.

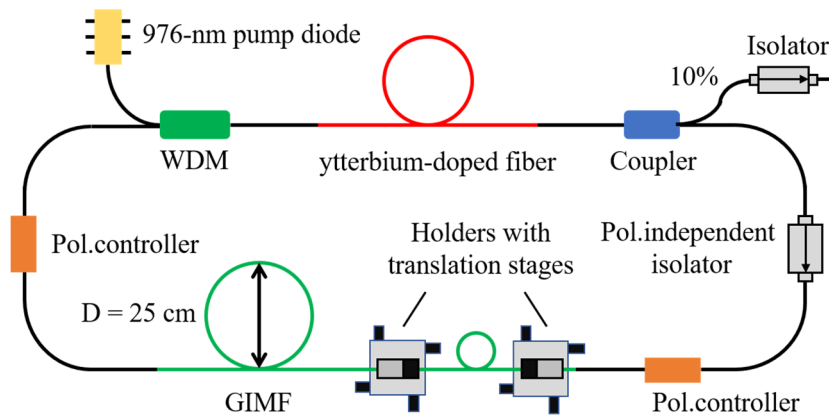


Fig. 4. Experimental setup of the tunable mode-locked ytterbium-doped fiber laser based on NL-KBC. WDM: wavelength division multiplexer; GIMF: graded-index multimode fiber; Pol.: polarization; D: diameter.

The characteristics of output laser were detected by an optical spectrum analyzer (MS9740A, Anritsu), an oscilloscope (DPO5204B, Tektronix) together with a high-speed photodetector (DET08C/M, Tektronix), a radio-frequency analyzer (RSB206b, Tektronix) and an autocorrelator (PulseCheck USB, APE). When the short GIMF segment was adjusted to a specific bending condition, the self-starting mode-locked operation could be achieved with only increasing the pump power. For example, when the operating central wavelength was tuned to 1040 nm, the single-pulse mode-locked state was obtained at the threshold of 60 mW. With the pump power increasing to 160 mW, stable mode-locked state could be maintained and its output pulse characteristics was measured. The output pulse trace and radio-frequency (RF) spectrum are presented in Fig. 5. The period of laser pulses was measured to be about 36 ns, and the first peak of RF spectrum was centered at 27.566 MHz, corresponding to the cavity length of 7.4 m. The signal-to-noise ratio of this RF spectrum was measured to be 75 dB; no multi pulse or harmonic mode-locked signals were found in 700-MHz-span RF spectrum. These results further confirmed that the laser was operating at a stable single-pulse mode-locked state.

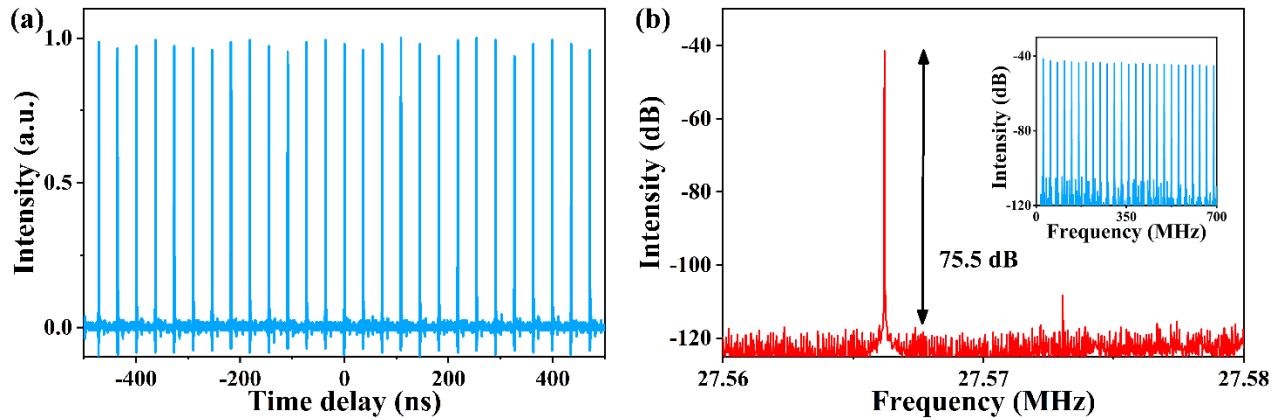


Fig. 5. (a) Single-pulse mode-locked pulse train when the pump power was 160 mW. (b) The output radio frequency spectrum with 10 kHz span and 1 Hz resolution bandwidth. Inset: The output radio frequency spectrum with 700 MHz span and 100 Hz resolution bandwidth.

Fig. 6(a) shows the laser output spectrum at the same pump power of 160 mW; its central wavelength was 1040 nm with a 20-dB bandwidth of 6.2 nm. The spectrum presented a cat-ear-like trace, which is a typical characteristic of dissipative soliton from all-normal-dispersion fiber lasers. Besides, the autocorrelation trace of output pulse was also measured (the inset of Fig. 6(b)); assuming a Gaussian pulse shape, the pulse duration could be calculated to 25.7 ps. It could be compressed externally to 791 fs using a single 1200-line/mm grating.

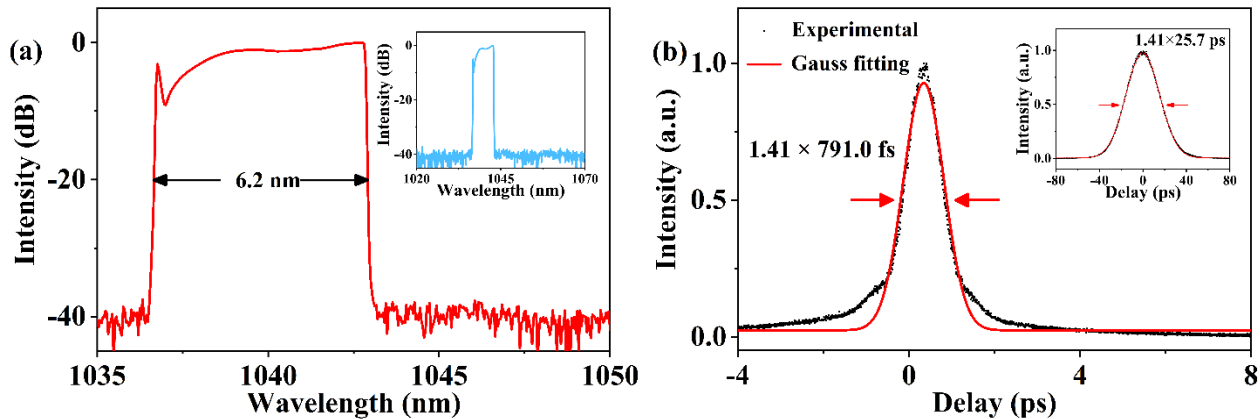


Fig. 6. (a) The output optical spectrum with a spectral resolution of 0.04 nm and a span range of 15 nm; inset: the output optical spectrum with a spectral resolution of 0.1 nm and a span range of 50 nm. (b) The autocorrelation trace of dechirped output pulses with Gaussian fitting; inset: the autocorrelation trace of output pulses with Gaussian fitting.

In addition, tunable mode-locked operation was studied in this laser. By adjusting the translation stages, different bending condition of GIMF can be achieved. As a result, the central wavelength of output laser could be tuned from 1032 nm to 1066 nm while the stable mode-locking state could be maintained. The output spectra with different central wavelength are presented in Fig. 7. They all showed a cat-ear-like trace, but their mode-locked thresholds are different ranged from 60 mW to 330 mW. The spectral tuning range of the mode-locked operation may be limited by the gain bandwidth of the ytterbium-doped fiber or band-pass filter effect induced by other fiber devices. Moreover, in some specified cases during the tuning process, the mode-locked operation together with continuous-wave components occurred (as shown in Fig. 7). In these cases, we suppose that two or more peaks could be found in the feature of the FM energy proportion versus wavelength at the end of GIMF (such as the case in Fig. 2(c) and 2(d)). Therefore, the SA transmittance of two or more wavelengths was similar without a dominant

or maximum one. Together with the gain bandwidth and other band-pass filter effects, mode locked operation could be achieved at one wavelength while continuous-wave lasing was achieved at other wavelengths. Nevertheless, laser operation in these cases also had good stability, and it could maintain mode-locked state for several hours. The phenomena of tunable laser output and multiple lasing wavelengths mentioned above can be inferred by the simulation results, which verified the validity of our numerical model in Section 2. Table 1 illustrates the realization methods and tuning ranges of different tunable mode-locked lasers. Compared with those commercial tuning methods, no additional spectral filters are required but similar tuning range can be achieved in our laser.

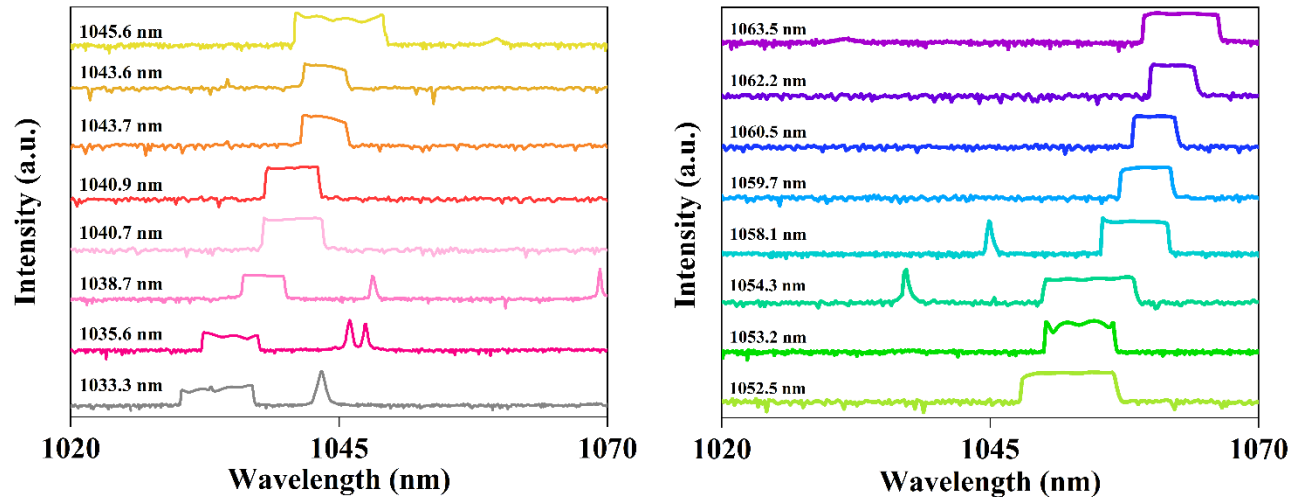


Fig. 7. Output spectra of the tunable mode-locked fiber laser with central wavelength ranged from 1033.3 nm to 1063.5 nm.

Table 1. Tuning properties of different tunable mode-locked fiber lasers

| Mode-locking method | Tuning element | Tuning range |
|------------------------------------|---|------------------------------|
| Single walled carbon nanotubes [8] | Spectral filter | 1032-1062 nm |
| Graphene saturable absorber [9] | Chirped Bragg grating | 1539-1542 nm or 1545-1550 nm |
| Dissipative four wave mixing [10] | Fourier domain programmable optical processor | 1535-1565 nm |
| SA based on NL-KBC in this article | Graded-index multimode fiber in the SA | 1033-1063nm |

4. Conclusion

In conclusion, we have demonstrated a novel all-fiber tunable mode-locked laser with a SA based on NL-KBC effect. The mechanisms of tunable band-pass filter and saturable absorption effects in the SA have been studied by an original numerical model. Guided by the simulation results with adjusting the bending condition of GIMF, the laser could produce stable dissipative soliton pulses with tunable central wavelength ranged from 1033 nm to 1063 nm. This work provides a novel approach for constructing wavelength tunable mode-locked fiber lasers which can be used in optical communication, optical sensing and other important fields. Future works will focus on the all-polarization-maintaining-fiber configuration and precise tuning of the mode-locked wavelength in these lasers.

Funding. National Natural Science Foundation of China (11832019, 11472313, 11572355); Natural Science Foundation of Guangdong Province (2018A030310092).

Acknowledgment. The authors would like to acknowledge Zhanwei Liu for the helpful discussion on the numerical model and fine guidance on the MPA program. We also acknowledge Ugur Tegin for helpful discussion on the laser design, and Yu Duan of Emgo-tech Ltd (Zhuhai), Fujuan Wang, Jiaoyang Li for the technical support in this work.

References

1. S. Yang, Z. Li, H. Zhang, S. Yuan and X. Dong, "Wavelength Tunable Dual-Wavelength Actively Mode-Locked Fiber Laser with F-P LD as Modulator," *Acta Optica Sinica*, 23, 472(2003)
2. D. Zhang, J. Zhao, Q. Yang, Wen Liu, Y. Fu, C. Li, M. Luo, S. Hu, Q. Hu, and L. Wang, "Compact MEMS external cavity tunable laser with ultra-narrow linewidth for coherent detection," *Optics Express*, 20,19670-19682(2012).
3. J. P. Besson, S. Schilt, and L. Thévenaz, "Multi-gas sensing based on photoacoustic spectroscopy using tunable laser diodes," *Spectrochim Acta A Mol Biomol Spectrosc*, 60, 3449-3456(2004).
4. K. M. Busa, and M. S. Brown. "Fast Data Processing for Optical Absorption Measurements." *AIAA Aerospace Sciences Meeting* (2015).
5. N. Deguil, E. Mottay, F. Salin, P. Legros and D. Choquet, "A novel diode-pumped tunable system for multi-photon microscopy," *Microscopy research and technique*, 63, 23-26(2004).

6. S. Yin, T. Chan and W. I. Way, "100 km DWDM Transmission of 56 Gb/s PAM4 per λ via Tunable Laser and 10 Gb/s InP MZM," *IEEE Photonics Technology Letters*. 27, 2531-2534(2015).
7. F. Wang, A. G. Rozhin, V. Scardaci, Z. Sun, F. Hennrich, I. H. White, W. I. Milne and A. C. Ferrari, "Wideband-tuneable, nanotube mode-locked, fibre laser," *Nature Nanotechnology*. 3, 738-742(2009).
8. Y. Senoo, N. Nishizawa, Y. Sakakibara, K. Sumimura, E. Itoga, H. Kataura and K. Itoh, "Polarization-maintaining, high-energy, wavelength-tunable, Er-doped ultrashort pulse fiber laser using carbon-nanotube polyimide film," *Opt. Express*. 17, 20233-20241(2009).
9. X. He, Z. Liu and D. N. Wang, "Wavelength-tunable, passively mode-locked fiber laser based on graphene and chirped fiber Bragg grating," *Opt. Lett.* 37, 2394-2396(2012).
10. J. Schröder, T. D. Vo, B. J. Eggleton, "Repetition-rate-selective, wavelength-tunable mode-locked laser at up to 640 GHz," *Opt. Lett.* 34, 3902-3904(2009).
11. K. Krupa, A. Tonello, B. M. Shalaby, M. Fabert, A. Barthélémy, G. Millot, S. Wabnitz, and V. Couderc, "Spatial beam self-cleaning in multimode fibres," *Nature Photonics*. 11, 237 (2017).
12. Z. Liu, L. G. Wright, D. N. Christodoulides and F. W. Wise, "Kerr self-cleaning of femtosecond-pulsed beams in graded-index multimode fiber," *Opt. Lett.* 41, 3675-3678(2016).
13. B. Zhang, S. Ma, Q. He, J. Guo, Z. Jiao and B. Wang, "Investigation on saturable absorbers based on nonlinear Kerr beam cleanup effect," *Opt. Express*. 28, 6367-6377(2020).
14. B. Zhang, S. Ma, S. Lu, Q. He, J. Guo, Z. Jiao and B. Wang, "All-fiber mode-locked ytterbium-doped fiber laser with a saturable absorber based on the nonlinear Kerr beam cleanup effect," *Opt. Lett.* 45, 6050-6053(2020).
15. H. F. Taylor, "Bending effects in optical fibers," *Journal of Lightwave Technology*. 2, 617-628(1984).
16. Y. H. Sohn. "Light propagation in multimode graded-index optical fibers undergoing bending," Doctoral dissertation (2002). <https://search.proquest.com/dissertations/docview/305439550/32799DAA61B042FDPQ/1?accountid=14167>
17. L. G. Wright, Z. M. Ziegler, P. M. Lushnikov, Z. M. Zhu, M. A. Eftekhari, D. N. Christodoulides and F. W. Wise, "Multimode Nonlinear Fiber Optics: Massively Parallel Numerical Solver, Tutorial and Outlook," *IEEE Journal of Selected Topics in Quantum Electronics*. 24, 1-16(2018).